Application of the all-speed method to steady and unsteady flows on unstructured grids

Wladimyr M. C. Dourado – dourado@lcd.ensma.fr
Centro Técnico Aeroespacial, Instituto de Aeronáutica e Espaço
CTA/IAE/ASA-P, 12228-904 – São José dos Campos – SP – BRASIL
João Luiz F. Azevedo – azevedo@iae.cta.br
Centro Técnico Aeroespacial, Instituto de Aeronáutica e Espaço
CTA/IAE/ASE-N, 12228-904 – São José dos Campos – SP – BRASIL
Pascal Bruel – bruel@lcd.ensma.fr
Centre National de la Recherche Scientifique
Laboratoire de Combustion et de Détonique
BP 40109 - 86961 Futuroscope Chasseneuil Cedex – FRANCE

Abstract. *A numerical method based on the all-speed approach is proposed to calculate low Mach number separated and unsteady flows. The Navier-Stokes equations are solved on hybrid and non-hybrid unstructured meshes. The results are compared with analytical solutions and experimental data available in the literature.*

Key Words: *Aerodynamics, All speed methods, Finite volume method, Unstructured grids, Recirculating flows, Unsteady flows.*

1. INTRODUCTION

Among the numerous numerical methods than can be considered to deal with low Mach number flows (Chorin, 1967; Chang and Kwak, 1984; Bruel, Karmed and Champion, 1996), the all speed method, proposed by Dourado and Azevedo (1999) has proved to be able to deal with both internal and external steady flows. The objective of the present study is to validate this method for both viscous and unsteady flows. To do so, the proposed algorithm is applied

to calculate i) the laminar confined flow past a backward facing step and ii) the flow over an oscillating plate (second Stokes' problem). In the former case, a special attention is devoted to the use of an hybrid mesh which combines triangular control volumes in the recirculating zones and quadrangular elements elsewhere, following in that respect the approach proposed by Dourado and Azevedo (1999) in the case of boundary layer flows.

2. THEORETICAL AND NUMERICAL FORMULATION

Only a brief overview of the all speed method is given here. A detailed description can be found in Dourado and Azevedo (1999; 1996) and Martins (1994). The 2-D Navier-Stokes equations are considered in the present study, namely:

$$\int_V \frac{\partial Q}{\partial t} dV + \oint_S \left(E_e \vec{i} + F_e \vec{j}\right) \cdot \vec{n} dS = \oint_S \left(E_v \vec{i} + F_v \vec{j}\right) dS \ , \tag{1}$$

where Q is the vector of unknowns i.e.:

$$Q = \{\rho, \rho u, \rho v, e\}^T \ , \tag{2}$$

E_e and F_e are the convective fluxes and E_v and F_v are the viscous terms, respectively. These equations are supplemented by the gasdynamic equation for the total energy e given by:

$$e = \frac{p}{\gamma - 1} + \frac{1}{2}\rho\left(u^2 + v^2\right) \ , \tag{3}$$

where p is the static pressure, ρ is the density, u and v are the Cartesian components of the velocity vector and γ is the adiabatic coefficient of gas. The main idea behind the all-speed method (Dourado and Azevedo (1999; 1996), Martins (1994) and Chen and Pletcher (1991)) is to change the set of dependent variables from Q to $q = \{p, u, v, T\}^T$ where T is the temperature. Thus, adopting this strategy implies that Eq. 1 has to be re-written as:

$$\int_V \mathcal{D} \frac{\partial q}{\partial t} dV + \oint_S \left(E_e \vec{i} + F_e \vec{j}\right) \cdot \vec{n} dS = \oint_S \left(E_v \vec{i} + F_v \vec{j}\right) dS \ , \tag{4}$$

where $\mathcal{D} = \partial Q / \partial q$ is the Jacobian matrix associated with the change of variables. Finally, Eq. 4 is dealt with by using a strategy adapted to unstructured grids that can be either hybrid (triangles and quadrangles) or of a single type (triangles or quadrangles). In the latter case, the numerical treatment of Eq. 4 is similar to that reported by Dourado and Azevedo (1999; 1996) and Mavriplis (1990). The solution is advanced in time by using a five-stage second-order Runge-Kutta method. The recourse to hybrid meshes (Mavriplis (1998; 1995)) is justified whenever the regions of the flow where large gradients are present possess a preferential direction as it is the case for instance, for boundary layer flows.

For such hybrid meshes, it is necessary to explain how the unstructured mesh technique, relying on an edge-based data structure is implemented in a cell vertex unstructured grid

context. In the framework of the present finite volume approach, a control volume must be defined around each node at which the balance equations are solved. To be more specific, let us consider the node j shown in Fig. 1, and which is surrounded by quadrangular elements. The control volume V_Qj associated with this node is defined by all these four quadrangular elements, and the related control surface is indicated in the figure with dotted lines. Similarly, control volumes V_Hi, V_Qk and V_hl can be defined around the nodes i, k and l. Considering now the edges that belong to the control surfaces, it appears that, for instance, the oriented edge referred to as $E1$ in Fig. 1 is shared by the triangular element placed "at the right" of this edge and by the quadrangular element located "at the left" of this edge. Consequently, the flux across $E1$ contributes to the flux balance of three control volumes, namely V_Qj, V_Qk and V_Hi, whereas for edge $E2$ which is shared by only two triangular elements, the edge flux contributes to the flux balance of two control volumes only, namely V_Hi and V_hl. Thus, the number of volumes which are influenced by each edge flux depends on the type of elements that are sharing that particular edge and is highly dependent on the grid topology.

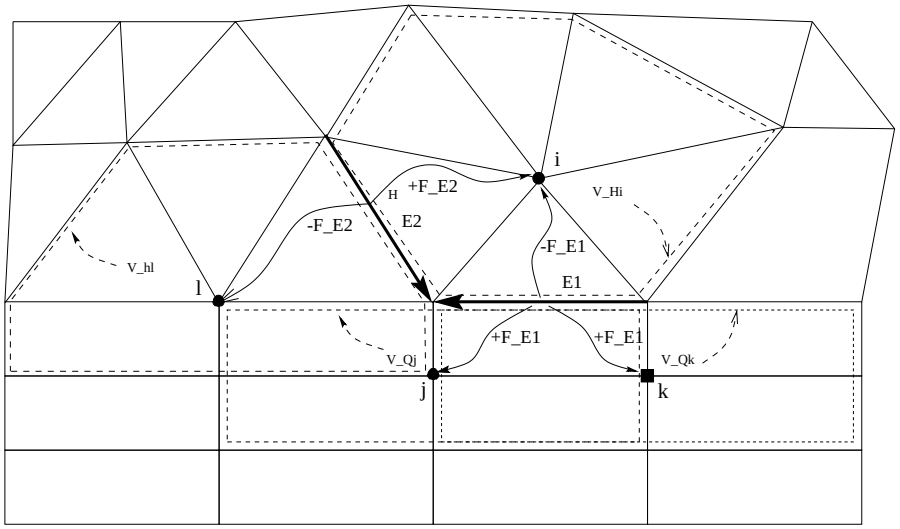

Figure 1: Example of edge-based, hybrid grid, flux calculation.

3. TEST CASES

3.1. Backward facing step flow

The first test case considered is the case of the laminar flow past a backward facing step studied experimentally by Armaly et al. (1983). For such a flow geometry, an hybrid mesh has been chosen because this flow is known to feature both boundary layer type regions and recirculating zones. Consequently, quadrangular elements are preferable in the former regions whereas triangular elements are more suited in the latter regions. An example of the hybrid mesh adopted to discretize the physical domain is shown in Fig. 2. The comparison

with the experimental results is performed for a Reynolds number value equal to 400 based on the inlet channel height and the inlet bulk velocity.

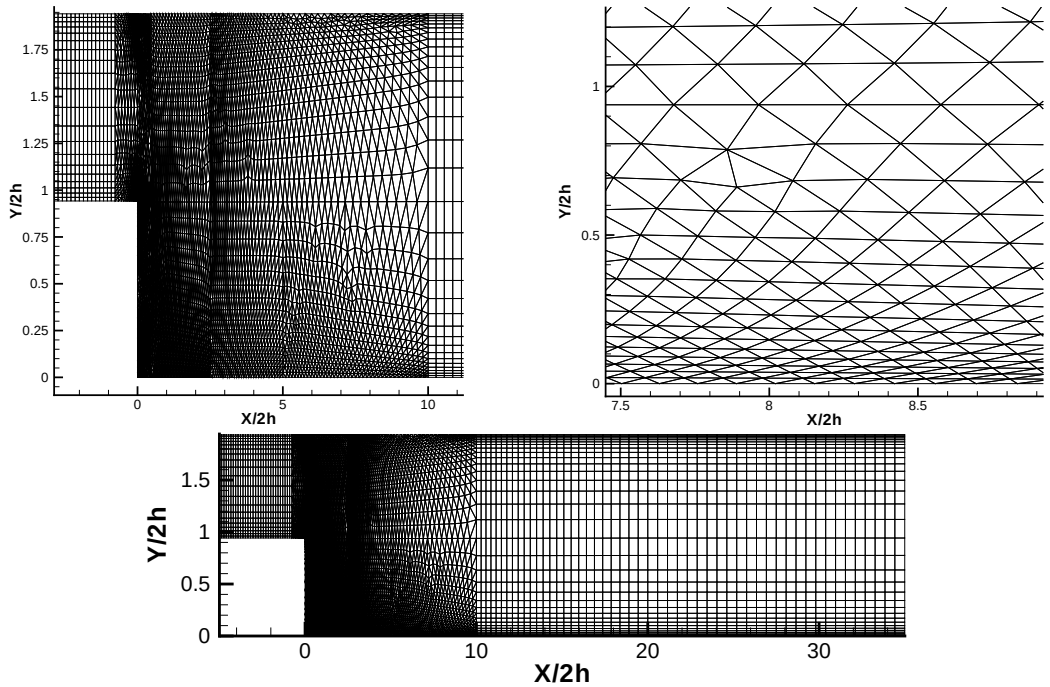

Figure 2: Backward facing step flow: Details of the 6001-node and 9297-element hybrid mesh ($h = 5.2$ mm).

The size of the computational domain is the same as the one chosen by Armaly et al. (1983) for the numerical part of their study. This corresponds to an inlet channel length equal to five reference length and an outlet channel length equal to thirty-five reference length, the reference length being taken equal to the inlet channel height ($h = 5.2$ mm). A parabolic Poiseuille-like velocity profile and a constant temperature are imposed at the entrance of the inlet channel, with a Mach number equal to 0.05. No-slip conditions are imposed at the solid walls and a fixed pressure level, $p_{outlet} = p_{ref}$ is prescribed at the channel outlet section where the other variables are extrapolated. Finally, the flow is considered to be initially at rest.

3.2. Second Stokes' problem

The unsteady flows represent another class of flows that are of considerable interest in the engineering field. Along these lines, we have investigated the capabilities of the present numerical scheme to cope with a flow unsteadiness by assessing its capability to predict the time varying velocity field generated by an oscillating plate (Second Stokes' problem) for which there exists an analytical solution given by (Schlichting, 1979):

$$U_a\left(u,t\right) = U_0 * e^{-\eta} * \cos\left(n * t - \eta\right) \tag{5}$$

with the dimensionless variable η defined by:

$$\eta = y\sqrt{\frac{n}{2 * \nu}}\ , \tag{6}$$

where $n = 2 * \pi * f$, y is the coordinate normal to the plate, f the frequency of oscillation, U_0 the maximum velocity amplitude and t the time. For all cases, U_0 is taken equal to 1.0 m/s. Four different values of the frequency f of the plate oscillation have been considered i.e. 10, 100, 200 and 500 Hz. Examples of the meshes used for such a case are given in Fig. 3.

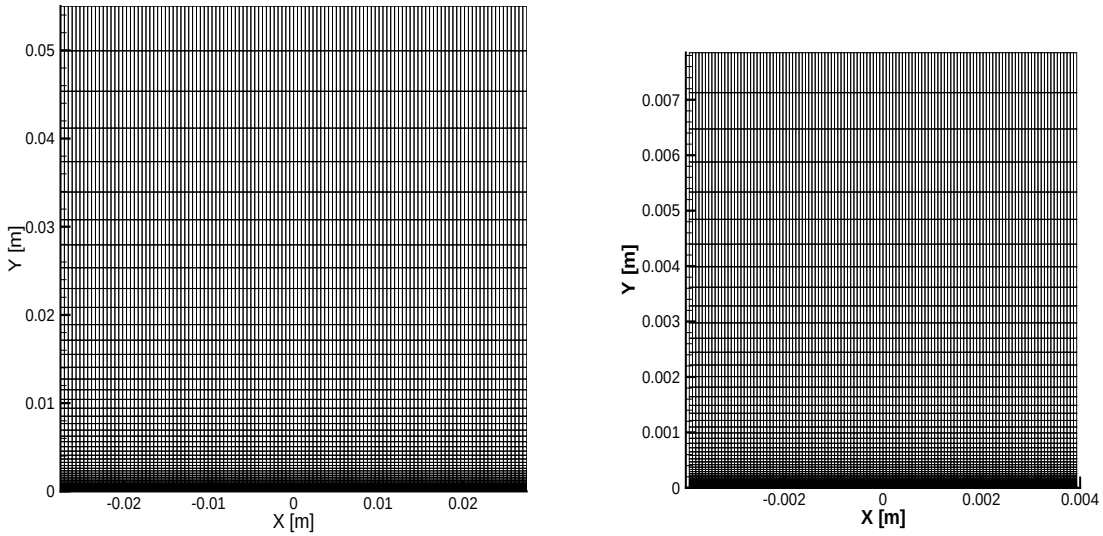

Figure 3: Second Stokes' problem, view of the two 121x49-node meshes used: left "Mesh 1", for $f = 10$, 100, 200 and 500 Hz; right "Mesh 2", for $f = 500$ Hz.

Periodic boundary conditions are used in the direction of the plate oscillation, a no slip condition is enforced at the plate and the flow is supposed to be at rest at the upper boundary. Finally, stagnation conditions are taken as initial conditions.

In both test cases, the fluid used is air, the initial pressure and the temperature are $p_{ref} = 1.01325 \times 10^5\ Pa$ and 288 K, respectively. Under these conditions, the fluid kinematic viscosity is equal to $1.44 \times 10^{-5} m^2/s$.

All meshes used in this work have been generated by the EMC^2 software (Saltel and Hecht, 1995) which is able to generate fully unstructured hybrid grids.

4. RESULTS

4.1. Backward facing step flow

The vectors velocity plot together with the associated streamlines are shown in Fig. 4, where it is possible to see in detail the re-attachment region. A quadrilateral elements in the boundary layer of the recirculation zone has been also tested without any significant

influence on the velocity field and thus a fully triangular grid has been retained for this zone. The dimensionless value of the streamwise abscissa of the reattachment point obtained with the present calculations is $X = 7.76$ to be compared with the value of $X = 8.36$ obtained by Armaly et al. (1983). This corresponds to a difference of 7.8% in the re-attachment point location, which can be considered as a good result for the present calculations. The recirculation region near the step corner, which is particularly difficult to detect, is well captured by the present algorithm. The corresponding pressure contours associated with the velocity field are shown in Fig. 5, where it is possible to see the pressure drop captured by the method and the smooth pressure distribution observed far from the step corner. The pressure oscillations are very weak and do not influence significantly the converged solution.

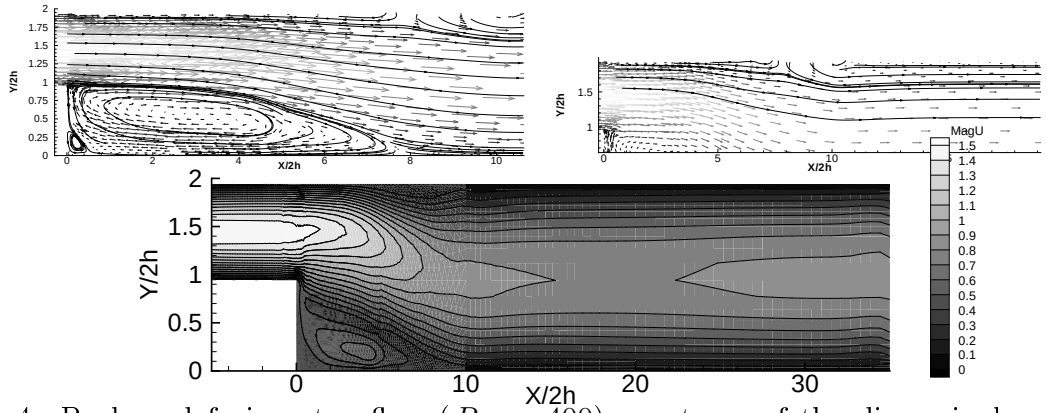

Figure 4: Backward facing step flow ($Re = 400$): contours of the dimensionless velocity $\vec{U}/u_{ref}$ and related streamlines ($u_{ref} = 17$ m/s).

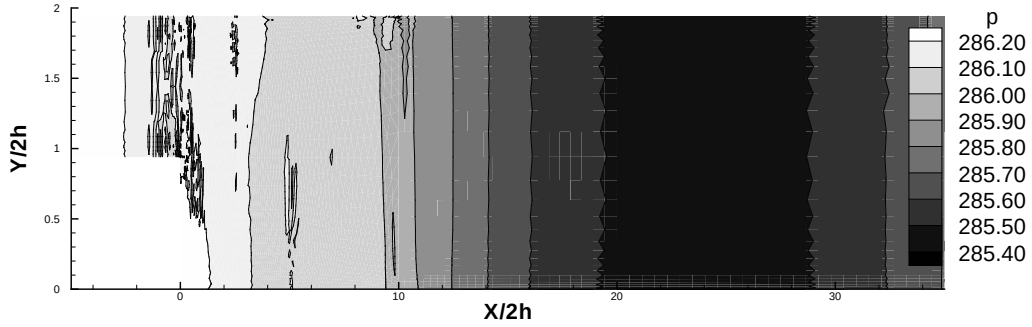

Figure 5: Backward facing step flow ($Re = 400$): dimensionless pressure contours ($p = \tilde{p}/\rho_{ref}u_{ref}^2$).

These limited but encouraging comparisons show clearly that the all-speed method combined with an hybrid mesh approach is able to capture the gross properties of a separated flow, thus extending the variety of flows that this method can deal with.

4.2. Second Stokes' problem

A comparison between the analytical solution and the numerical results, obtained with the same mesh ("mesh 1"), are presented in Figs. 6 and 7. The comparison with the analytical

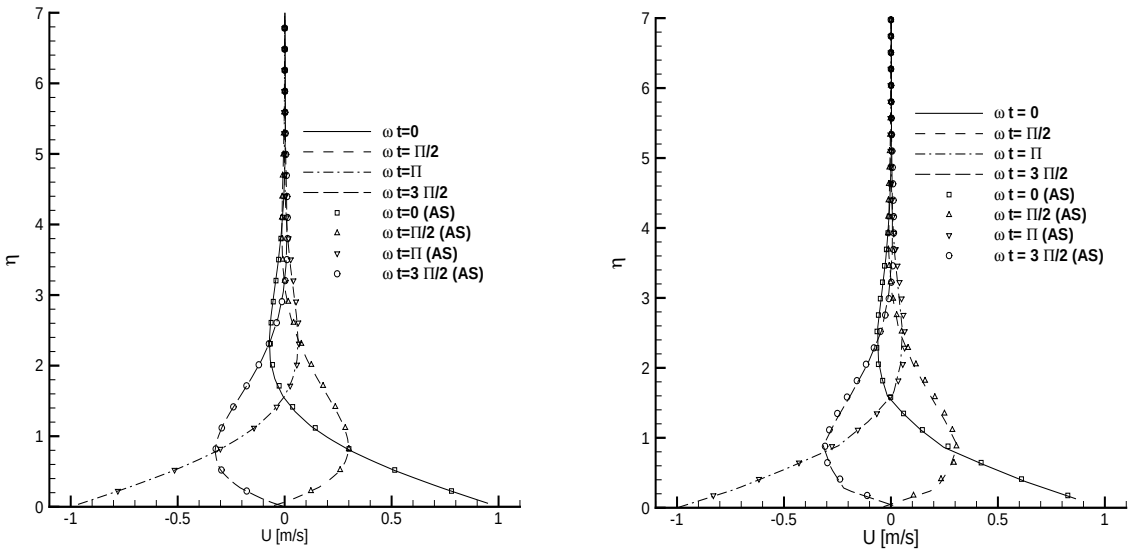

Figure 6: Second Stokes' problem, velocity profiles for some phase angles: left, for $f = 10$ Hz; right, for $f = 100$ Hz (mesh 1).

solution are performed when one complete cycle of oscillation has been completed in order to avoid any interference that could stem from the transient evolution associated with the prescription of the initial conditions. A good agreement is observed, especially for the low frequency cases for which the diffusion layer is correctly resolved.

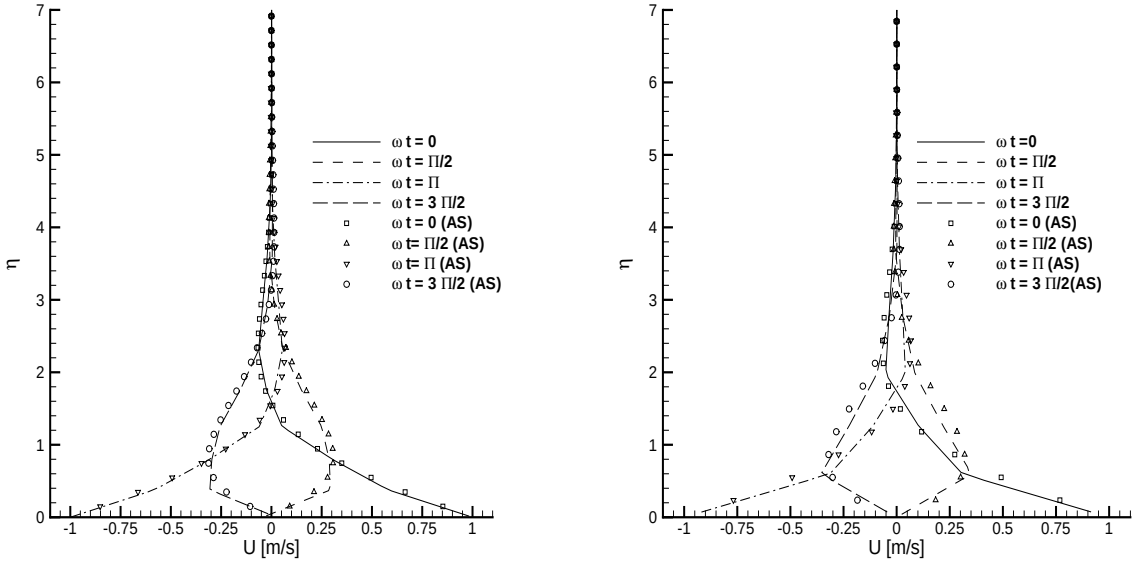

Figure 7: Second Stokes' problem, velocity profiles for some phase angles: left, for $f = 200$ Hz; right, for $f = 500$ Hz (mesh 1).

The accuracy of the numerical solution is becoming poor when f increases (Fig. 7) because, in that case, the thin associated diffusion layer, which is becoming thinner, is not resolved properly by the mesh. Consequently, in order to resolve properly this thinner diffusion layer a new mesh has been used ("mesh 2") with the same number of elements as "mesh 1" but with a larger refinement in the vicinity of the plate to obtain the same layer element density as the one obtained previously with "mesh 1" for $f = 10$ Hz. The results obtained with this

new mesh for $f = 500$ Hz (Fig. 8) put into evidence, again, a very good agreement between the analytical solution and the numerical results.

Such a sensitivity of the accuracy of the numerical solution to the mesh density is illustrated in Fig. 9 by the evolution of the residue L defined by:

$$L = \sqrt{\sum_{i=1}^{\mathrm{nn}} |U_a - U_{n_i}|^2} \ , \tag{7}$$

where nn is the total number of nodes of the mesh, U_a is the analytical solution given by "Eq. (5)" and U_n is the numerical solution. For "mesh 1", the residue appears to be an increasing function of the frequency f. With a refined mesh (mesh 2) a noticeable improvement of the accuracy of the solution is obtained as it is shown for a frequency $f = 500$ Hz of the plate oscillation.

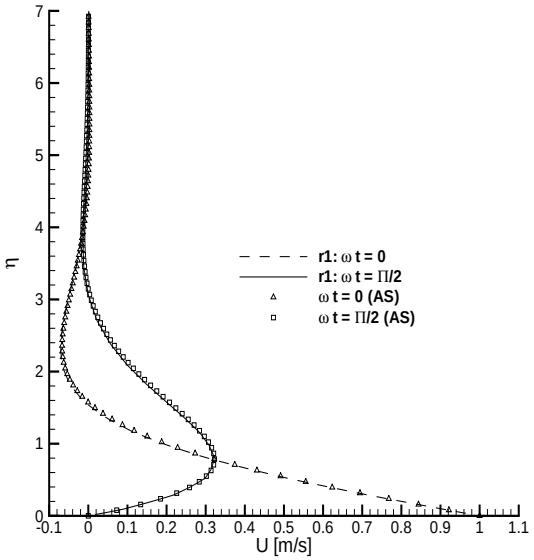

Figure 8: Second Stokes' problem, velocity profiles for some phase angles: for $f = 500$ Hz (mesh 2).

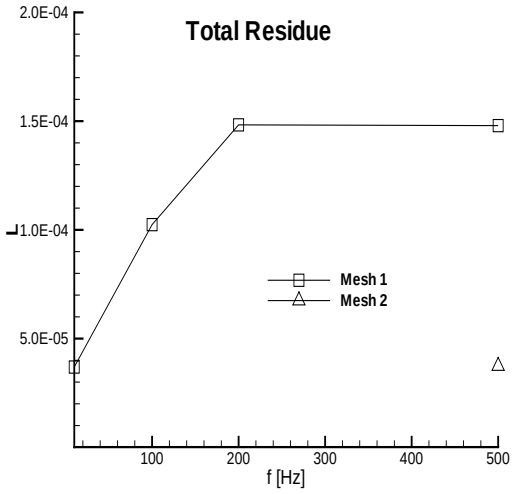

Figure 9: Second Stokes' problem: Total residue as a function of the frequency of the plate oscillation.

5. CONCLUDING REMARKS

The analysis of the results presented here shows that the all speed method is able to deal with fluid flows at very low Mach number. The spatial and the temporal accuracy of the proposed method is adapted to deal with separated flows and unsteady flows.

The drawback of this explicit time marching method is that it does not allow the use of a large value of the CFL number. This characteristic may cause a prohibitive computational overhead if one attempts to employ this method to accurately resolve low frequency physical phenomena. In that case, an implicit time marching procedure should be combined with the present all-speed approach.

References

Armaly, B. F., Durst, F., Pereira, J. C. F. and Schönung, 1983, *Experimental and theoretical investigation of backward-facing step flow,* J. Fluid Mechanics, Vol. 127, pp.473-496.

Bruel, P., Karmed, D. and Champion, M., 1996, *A pseudo-compressibility method for reactive flows at zero Mach number, Journal of Computational Fluid Dynamics,* Vol. 7, pp. 291-310.

Chang, J. L. C., and Kwak, D., 1984, *On the method of pseudo-compressibility for numerically solving incompressible flows,* AIAA paper 84-0252.

Chen, K.-H., and Pletcher, R. H., 1991, *Primitive variable, strongly implicit calculation procedure for viscous flows at all speeds* , AIAA Journal, Vol. 29, No. 8, Aug.

Chorin, A. J., 1967, *A numerical method for solving incompressible viscous flow problems* , Journal of Computational Physics, Vol. 2, pp. 12-26.

Dourado, W. M. C. and Azevedo, J. L. F., 1996, *Flow simulation with unstructured meshes over basic automotive configurations with all speed method,* Proceedings of the 6th Brazilian Congress of Engineering and Thermal Sciences and 6th Latin American of Mass and and Heat Transfer, ENCIT/LATCYM 96, November, Florianópolis, SC, Vol. I, pp. 553-558 (in Portuguese, original title is "Simulação de escoamentos com malhas não-estruturadas sobre configurações automotivas básicas com um método para toda a faixa de velocidade").

Dourado, W. M. C. and Azevedo, J. L. F., 1999, *Analysis of an all speed method in laminar flows using unstructured meshes,* 15th Brazilian congress of Mechanical Engineering, November 22-26, Águas de Lindóia, SP - Brazil, Proceeding in CD-ROM - ISBN # 85-85769-03-3.

Martins, J. M., 1994, *A finite difference method for flow simulation at all speeds,* Master Thesis, Instituto Tecnológico de Aeronáutica, São José dos Campos, SP, Brazil (in Portuguese, original title is "Um método de diferenças finitas para simulação de escoamentos em qualquer regime de velocidade").

Mavriplis, D., 1990, *Accurate multigrid solution of the Euler equations on unstructured and adaptive meshes,* AIAA Journal, Vol. 28, No. 2, pp. 213-221.

Mavriplis, D., 1995, *A unified multigrid solver for the Navier-Stokes equations on mixed element meshes,* AIAA Paper 95-1666.

Mavriplis, D., 1998, *Multigrid strategies for viscous flow solvers on anisotropic unstructured meshes,* Institute for Computer Applications in Science and Engineering (ICASE) Rept. 98-6.

Saltel, E. and Hecht, F., 1995, *EMC*^{2} *Un logiciel d'édition de maillages et de contours bidimensionnels,* Institut National de Recherche en Informatique et en Automatique (INRIA), Technical Report N. 118, October.

Schlichting, H., 1979, *Boundary-Layer Theory,* McGraw-Hill, 7th Ed.